Journal of Applied Fluid Mechanics, Vol. 10, No. 3, pp. 915-924, 2016.
Available online at www.jafmonline.net, ISSN 1735-3572, EISSN 1735-3645.
DOI: 10.18869/acadpub.jafm.73.240.24008

Non-Uniform Heat Source/Sink and Thermal Radiation Effects on the Stretched Flow of Cylinder in a Thermally Stratified Medium

T. Hayat[1,3], Sadia Asad[2†] and A. Alsaedi[3]

[1]*Department of Mathematics, Quaid-i-Azam University 45320, Islamabad 44000, Pakistan*
[2]*COMSATS Institute of Information Technology, Wah Cantt 47040, Pakistan.*
[3]*Nonlinear Analysis and Applied Mathematics (NAAM) Research Group, Department of Mathematics, Faculty of Science, King Abdulaziz University,Jeddah 21589, Saudi Arabia*

†Corresponding Author Email: asadsadia@ymail.com

(Received August 31, 2014; accepted October 7, 2015)

ABSTRACT

The paper addresses the influence of non-uniform heat source/sink in flow of couple stress fluid by a stretching cylinder in a thermally stratified medium. Thermal radiation effect in heat transfer analysis is also accounted. Conservation laws of mass, linear momentum and energy leads to nonlinear situation. Use of adequate transformations coverts the partial differential equations into the ordinary differential equations. Series solutions of the resulting equations are obtained for the velocity and temperature. Convergence of the solutions is explicitly checked. Impacts of various sundry variable son the velocity, temperature, wall shear stress and Nusselt number are examined through graphical illustrations and numerical values. The effect of β and Re on velocity field is qualitatively similar. For larger values of curvature parameter γ velocity enhances. Influences of S and R on temperature on the temperature distribution are opposite. Heat transfer at the surface decays when A and B increase.

Keywords: Couple stress fluid; Thermal radiation; Non-uniform heat source/sink and thermally stratified medium.

1. INTRODUCTION

The stretched flow in presence of heat transfer is quite prevalent in several engineering processes such as in extrusion, melt spinning, hot rolling, wire drawing, manufacture of plastic and rubber sheets, glass fiber production, paper production, food processing, manufacture of polymer sheets and in the movement of biological fluids. It is now recognized that fluids in such engineering applications are not viscous. Hence a new stage about non-Newtonian materials in the evolution of fluid dynamic theory is in progress during the past few decades. The flow behavior in shearing for such materials cannot be characterized by Newtons' law of viscosity. An intensive research effort, both theoretical and experimental, has been devoted in the past to problems of non-Newtonian fluids via different aspects. Different from the viscous fluids, the non-Newtonian liquids cannot be described by employing one constitutive relationship between the stress and rate of strain. This is because of diverse properties of non-Newtonian fluids in nature. Due to this fact several constitutive equations of Newtonian fluids exist. The additional rheological parameters in such constitutive equations lead to the complexities in the resulting differential equations. Generally the differential equations in non-Newtonian fluids are more subtle, higher order and complicated than the Navier-Stokes equations. The corresponding differential systems involving non-Newtonian fluids offer interesting challenges to the modelers, computer scientists and mathematicians from different quarters. One may mention few relevant recent studies on this topic by Khan *et al.* (2014).

Although the flow and heat transfer due to a stretching cylinder is important in wire drawing, hot rolling and fiber production but very less emphasis is given in this direction. The steady laminar flow caused by a stretching cylinder immersed in an incompressible viscous fluid with prescribed surface heat flux is investigated by Bachok and Ishak (2010) The authors computed the numerical solution in this study. Hydromagnetic flow by a permeable cylinder with heat and mass transfer has been reported by Chamkha (2011). He considered the problem in the presence of heat generation/absorption, chemical reaction and uniform transverse magnetic field. Mukhopadhyay

(2012) presented mixed convection flow of viscous incompressible fluid and heat transfer towards a stretching cylinder embedded in porous medium. An unsteady mixed convection boundary layer flow over a permeable non-linearly stretching vertical cylinder has been considered by Patil *et al*. (2012). They considered combined effects of buoyancy force and thermal diffusion in the presence of surface mass transfer. Effect of uniform magnetic field on slip flow by a stretching cylinder is examined by Mukhopadhyay (2013).

Moreover, the study of heat transfer in the presences of thermal stratification is of considerable importance in geological transport, geothermal system, power plant condensation systems and volcanic flows. Stratification of the medium may arise due to a temperature difference which gives rise to a density variation in the medium. This is known as thermal stratification and it usually arises due to thermal energy input into the medium from heated bodies and thermal sources. Thermal stratification is a characteristic of all fluid bodies surrounded by differentially heated side walls. Analysis for the axisymmetric laminar boundary layer mixed convection flow of an incompressible viscous fluid towards a stretching cylinder immersed in a thermally stratified medium has been given by Mukhopadhyay and Ishak (2012). MHD boundary layer flow and heat transfer by an exponentially stretching sheet embedded in a thermally stratified medium are studied by Mukhopadhyay (2013). Murthy *et al*. (2013) investigated the flow, heat and mass transfer in a thermally stratified nanofluid with convective boundary condition. Paolucci and Zikoski (2013) investigated the free convective flow along a heated vertical wall immersed in a thermally stratified environment.

Areas arises at high temperatures and acquaintance of radiative heat transfer becomes very vital for design of relevant equipment. For production of plastic sheets, gas turbines, missiles, space vehicles aircraft, nuclear power plants, satellites and foils. Slip flow of electrically conducting fluid with thermal radiation has been analyzed by Mukhopadhyay (2015). Flow and heat transfer analysis of MHD fluid in the presence of a uniform magnetic field with thermal radiation are investigated by Chaudhary *et al*. (2015). Sahu and Mishra (2015) reported radiative flow of a dusty fluid past a vertical stretching surface. Numerical study of boundary layer flows with heat transfer has been presented by Gireesha *et al*. (2015). They also take the effects of thermal radiation, Darcy porous medium and non-uniform heat source/sink. Theoretical influence of buoyancy and thermal radiation on magnetohydrodynamic flow past a stretching porous sheet has been studies by Daniel and Daniel (2015).

The main purpose of present attempt is to investigate the flow and heat transfer characteristics by a stretching cylinder immersed in a thermally stratified medium. Effects of thermal radiation and non-uniform heat generation are also considered. The flow equations are modeled for the constitutive relations of couple stress fluid. In fact the couple stress fluid shows the size dependent effect in the presence of couple stresses, body couples and non-symmetric stress tensor. The consideration of couple stress fluids has relevance in a number of processes that occur in industry such as the extrusion of polymer liquids, cooling of metallic plate in a bath, colloidal solutions, solidification of liquid crystals etc. The resulting nonlinear flow problem is solved by Homotopy analysis method (HAM) (Liao, 2009; Hayat, 2014; Hayat, 2013, Maleki, 2014; Rostami, 2014; Sheikholeslami, 2014; Farooq, 2015, Hayat, 2015). Results for velocity and temperature are graphically analyzed while the skin friction and local Nusselt number are examined through numerical values.

2. FORMULATION

We consider the steady two-dimensional flow of couple stress fluid embedded in a thermally stratified medium. Non-uniform heat source/sink and thermal radiation effects are present. The stretched cylinder is placed along the $x-axis$ and $r-axis$ is taken normal to it. The boundary layer equations comprising the conservation laws of mass, linear momentum and energy can be written as follows:

$$\frac{\partial(ru)}{\partial x}+\frac{\partial(rv)}{\partial r}=0, \tag{1}$$

$$\begin{aligned} u\frac{\partial u}{\partial x}+v\frac{\partial u}{\partial r}=\nu\left(\frac{\partial^2 u}{\partial r^2}+\frac{1}{r}\frac{\partial u}{\partial r}\right) \\ -\frac{\bar{\eta}}{\rho}\left(\frac{\partial^4 u}{\partial r^4}+\frac{2}{r}\frac{\partial^3 u}{\partial r^3}\right. \\ \left.-\frac{1}{r^2}\frac{\partial^2 u}{\partial r^2}+\frac{1}{r^3}\frac{\partial u}{\partial r}\right), \end{aligned} \tag{2}$$

$$\begin{aligned} \rho c_p\left[u\frac{\partial T}{\partial x}+v\frac{\partial T}{\partial r}\right]=k\frac{1}{r}\frac{\partial}{\partial r}\left(\frac{\partial T}{\partial r}\right) \\ -\frac{1}{r}\frac{\partial}{\partial r}(rq_r)+q'', \end{aligned} \tag{3}$$

in which ν is the kinematic viscosity, ρ is the fluid density, T is the fluid temperature, c_p is the specific heat, $q_r=-\frac{16\sigma^* T_\infty^3}{3k^*}\frac{\partial T}{\partial r}$ is the radiative heat flux, k^* is the mean absorption coefficient, σ^* is the Stefan-Boltzman constant, k is the thermal conductivity of the fluid and q'' is the rate of internal heat generations/absorption coefficient. The dimensionless from of q'' can be put in the form mentioned below [14]

$$q''=\left(\frac{kb}{\upsilon}\right)\left[A^*(T_w-T_\infty)+B^*(T-T_\infty)\right], \tag{4}$$

where A and B are parameters of space and temperature dependent internal heat generation/absorption respectively. It is noted that

the case $A>0$ and $B>0$ corresponds to internal heat generation while $A<0$ and $B<0$ holds for internal heat absorption, T_w is the temperature of sheet and T_∞ is the constant temperature for away from the sheet. The subjected boundary conditions are

$$u = U(x),\ v = 0,\ T = T_w \ \text{ at } r = a, \tag{5}$$

$$u \to 0,\ \frac{\partial u}{\partial r} \to 0\ \frac{\partial^2 u}{\partial r^2} \to 0\ T \to T_\infty \ \text{ as } r \to \infty. \tag{6}$$

In above equations $U(x) = U_0 x / l$ is the stretching velocity, $T_w(x) = T_0 bx / l$ is the prescribed surface temperature and $T_\infty(x) = T_0 cx / l$ is the variable ambient temperature. Further U_0 is the reference velocity, T_0 is the reference temperature, l is the characteristic length and *b* and *c* are the positive constants. Considering (Bachok and Ishak, 2010; Chamkha, 2011; Mukhopadhyay, 2012; Patil, *et al.* 2012; Mukhopadhyay, 2013; Mukhopadhyay and Ishak, 2012).

$$u = \frac{xU_0}{l} f'(\eta), \qquad v = -\frac{a}{r}\left(\frac{\upsilon U_0}{l}\right)^{\frac{1}{2}} f(\eta).$$

$$\theta(\eta) = \frac{T - T_\infty}{T_w - T_0}, \qquad \eta = \frac{r^2 - a^2}{2a}\left(\frac{U_0}{l\upsilon}\right)^{1/2} \tag{7}$$

Equation (1) is identically satisfied and Eqs. $(2-6)$ become

$$(1 + 2\eta\gamma) f''' + 2\gamma f'' - f'^2 + ff''$$
$$-8\beta Re\gamma^2 f''' + 8\gamma(1 + 2\eta\gamma) fiv\ \ (1 + 2\eta\gamma)^2 f^v \tag{8}$$

$$(1 + \frac{4}{3}R)\left[(1 + 2\gamma\eta)\theta'' + 2\gamma\theta'\right]$$

$$+ \Pr\left(f\,\theta' - f'\theta - Sf'\right) + Af' + B\theta = 0, \tag{9}$$

$$f = 0,\ f' = 1,\ \theta = 1 - S \ \text{ at } \eta = 0,$$

$$f' = f'' = f''' = 0,\ \theta = 0 \ \text{ as } \eta \to \infty, \tag{10}$$

Where

β=η̃/〖μa〗^2, dimensionaless couple stress parameter

R=(4〖〖σ^* T〗^3〗_∞)/(kk^*),Radiation parameter

S=c/b, Stratification parameter

γ =√(lυ/(a^2 U_0),) Curvature parameter

Pr=〖μc〗_p/k, Prandtl number

Re=(U_0 a^2)/υ, Reynold number

The wall shear stress is defined by

$$C_f = \frac{\tau_w}{\frac{1}{2}\rho U_w^2},\ \tau_w = \mu\left(\frac{\partial u}{\partial r}\right)_{r=a}$$

$$\text{or } \mathrm{Re}_x^{1/2} C_f = -f''(0). \tag{11}$$

Nusselt number Nu_x is given by

$$Nu_x = \frac{xq_w}{k(T_w - T_\infty)},$$

$$q_w = -k\left(1 + \frac{16\sigma^* T_\infty^3}{3k^* k}\right)\left(\frac{\partial T}{\partial r}\right)_{r=a}$$

$$\text{or } \mathrm{Re}_x^{1/2} Nu_x = -(1 + \frac{4}{3}R)\theta'(0). \tag{12}$$

3. SOLUTIONS

Initial guesses and auxiliary linear operators for the velocity and temperature fields are

$$f_0(\eta) = 1 - e^{-\eta},\ \ \theta_0(\eta) = (1 - S)e^{-\eta}, \tag{13}$$

$$£_f = f''' - f',\ \ £_\theta = \theta'' - \theta. \tag{14}$$

The properties satisfied by the operators are

$$£_f(C_1 + C_2 e^{\eta} + C_3 e^{-\eta}) = 0, \tag{15}$$

$$£_\theta(C_4 e^{\eta} + C_5 e^{-\eta}) = 0, \tag{16}$$

where C_i $(i = 1-5)$ are the constants.

The zeroth order deformation problems are represented by the following equations

$$(1-p)£_f\left[\hat{f}(\eta;p) - f_0(\eta)\right] = p\hbar_f \mathbf{N}_f\left[\hat{f}(\eta;p)\right], \tag{17}$$

$$(1-p)£_\theta\left[\hat{\theta}(\eta;p) - \theta_0(\eta)\right] = p\hbar_\theta \mathbf{N}_\theta\left[\hat{f}(\eta;p), \hat{\theta}(\eta,p)\right], \tag{18}$$

$$\hat{f}(0;p) = 0,\ \hat{f}'(0;p) = 1,\ \hat{f}'(\infty;p) = \hat{f}''(\infty;p) = 0, \tag{19}$$

$$\hat{f}'''(\infty;p) = 0,\ \ \hat{\theta}(0,p) = 1 - S,\ \ \hat{\theta}(\infty,p) = 0, \tag{20}$$

where $p \in [0,1]$ indicates an embedding parameter, h_f and h_θ are the non-zero auxiliary parameters and the nonlinear operators $\mathbf{N}_f$ and $\mathbf{N}_\theta$ are

$$\mathbf{N}_f[\hat{f}(\eta,p)] = (1 + 2\gamma\eta)\frac{\partial^3 \hat{f}(\eta,p)}{\partial\eta^3}$$
$$+2\gamma\frac{\partial^2 \hat{f}(\eta,p)}{\partial\eta^2} + \hat{f}(\eta,p)\frac{\partial^2 \hat{f}(\eta,p)}{\partial\eta^2}$$
$$-\left(\frac{\partial \hat{f}(\eta,p)}{\partial\eta}\right)^2$$
$$-\beta\,\mathrm{Re}\left(8\gamma^2\frac{\partial^3 \hat{f}(\eta,p)}{\partial\eta^3}\right.$$

$$+8(1+2\gamma\eta)\gamma\frac{\partial^4\hat{f}(\eta,p)}{\partial\eta^4}\Bigg) + (1+2\gamma\eta)^2\frac{\partial^5\hat{f}(\eta,p)}{\partial\eta^5},\Bigg) \tag{21}$$

$$\begin{aligned}\mathbf{N}_\theta[\hat{\theta}(\eta,p),\hat{f}(\eta,p)] = &\left(1+\frac{4}{3}R_d\right)\Big((1+2\gamma\eta)\\ &\frac{\partial^2\hat{\theta}(\eta,p)}{\partial\eta^2}+2\gamma\frac{\partial\hat{\theta}(\eta,p)}{\partial\eta}\Bigg)\\ &+\Pr\Bigg(\hat{f}(\eta,p)\frac{\partial\hat{\theta}(\eta,p)}{\partial\eta}\\ &-\hat{\theta}(\eta,p)\frac{\partial\hat{f}(\eta,p)}{\partial\eta}\Bigg)\\ &-S\frac{\partial\hat{f}(\eta,p)}{\partial\eta}\Bigg)\\ &+A\frac{\partial\hat{f}(\eta,p)}{\partial\eta}+B\hat{\theta}(\eta,p).\end{aligned} \tag{22}$$

For $p=0$ and $p=1$ we have the following equations

$$\hat{f}(\eta;0)=f_0(\eta),\quad \hat{\theta}(\eta,0)=\theta_0(\eta),$$

$$\hat{f}(\eta;1)=f(\eta),\quad \hat{\theta}(\eta,1)=\theta(\eta). \tag{23}$$

When p varies from 0 to 1 then $f(\eta,p)$ and $\theta(\eta,p)$ approach from $f_0(\eta),\theta_0(\eta)$ to $f(\eta)$ and $\theta(\eta)$. The series of the velocity and temperature fields through Taylor's expansion are chosen convergent for $p=1$ and thus

$$\begin{aligned}f(\eta) &= f_0(\eta)+\sum_{m=1}^{\infty}f_m(\eta),\\ f_m(\eta) &= \frac{1}{m!}\frac{\partial^m f(\eta;p)}{\partial\eta^m}\bigg|_{p=0},\end{aligned} \tag{24}$$

$$\begin{aligned}\theta(\eta) &= \theta_0(\eta)+\sum_{m=1}^{\infty}\theta_m(\eta),\\ \theta_m(\eta) &= \frac{1}{m!}\frac{\partial^m\theta(\eta;p)}{\partial\eta^m}\bigg|_{p=0}.\end{aligned} \tag{25}$$

The resulting problems at m^{th} order can be presented in the following forms

$$\pounds_f[f_m(\eta)-\chi_m f_{m-1}(\eta)]=\hbar_f\mathbf{R}_f^m(\eta), \tag{26}$$

$$\pounds_\theta[\theta_m(\eta)-\chi_m\theta_{m-1}(\eta)]=\hbar_\theta\mathbf{R}_\theta^m(\eta), \tag{27}$$

$$f_m(0)=f_m'(0)=f_m'(\infty)=f_m''(\infty)=0 \tag{28}$$

$$f_m'''(\infty)=\theta_m(0)=\theta_m(\infty)=0, \tag{29}$$

$$\begin{aligned}\mathbf{R}_f^m(\eta) = &(1+2\gamma\eta)f_{m-1}'''+2\gamma f_{m-1}''\\ &+\sum_{k=0}^{m-1}\left(f_{m-1-k}f_k''-f_{m-1-k}'f_k'\right)\\ &-\beta\,\mathrm{Re}\Big(8\gamma^2 f_{m-1}''''\\ &+8(1+2\gamma\eta)\gamma f_{m-1}'''''\Big)\\ &+(1+2\gamma\eta)^2 f_{m-1}''''''\Big),\end{aligned} \tag{30}$$

$$\begin{aligned}\mathbf{R}_\theta^m(\eta) = &\left(1+\frac{4}{3}R_d\right)\Big((1+2\gamma\eta)\theta_{m-1}''(\eta)\\ &+2\gamma\theta_{m-1}'\Big)+\Pr\sum_{k=0}^{m-1}\Big(\theta_{m-1-k}'f_k\\ &-f_{m-1-k}'\theta_k\Big)-\Pr Sf_{m-1}'\\ &+Af_{m-1}'+B\theta_{m-1},\end{aligned} \tag{31}$$

$$\chi_m=\begin{cases}0 & m\le 1\\ 1 & m>1\end{cases}.$$

The general solutions (f_m,θ_m) comprising the special solutions (f_m^*,θ_m^*) are

$$f_m(\eta)=f_m^*(\eta)+C_1+C_2e^{\eta}+C_3e^{-\eta}, \tag{32}$$

$$\theta_m(\eta)=\theta_m^*(\eta)+C_4e^{\eta}+C_5e^{-\eta}. \tag{33}$$

4. CONVERGENCE OF THE SOLUTIONS

Convergence of series solutions depends upon the non-zero auxiliary parameter $\hbar$. The auxiliary parameter $\hbar$ in Eqs. (24 and 25) can be regarded as an iteration factor that is widely used in numerical computations. It is well known that a properly chosen iteration factor can ensure the convergence of iteration. As pointed by Liao (2009), the valid region of $\hbar$ is a horizontal line segment parallel to horizontal axis. Figs. 3 and 4 witness that the admissible values of $\hbar_f$ and $\hbar_\theta$ are $-1.1\le\hbar_f\le-0.3$ and $-1.1\le\hbar_\theta\le-0.2$ respectively.

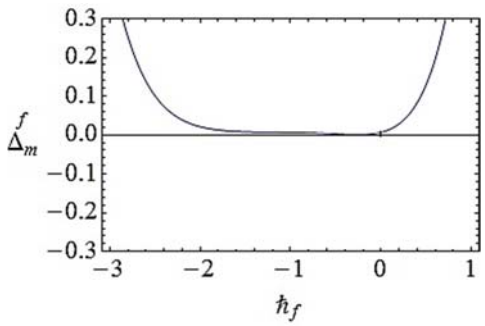

Fig. 1. Residual error for velocity field.

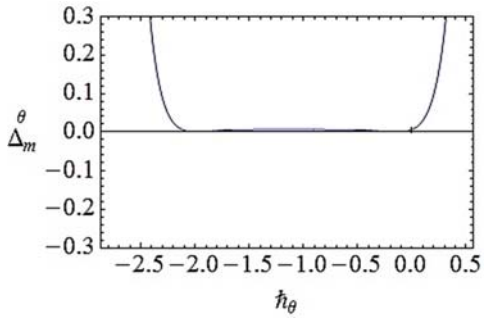

Fig. 2. Residual error for temperature fields.

These series solutions converge for the whole region of η when $\hbar_f = -0.7$ and $\hbar_\theta = -0.8$. Table 1 depicts the convergence of series solutions. It is confirmed here that 20^{th} -order approximations are enough for the convergence of velocity and temperature profiles. Fig. 1 and 2 show the residual error for velocity and temperature field respectively.

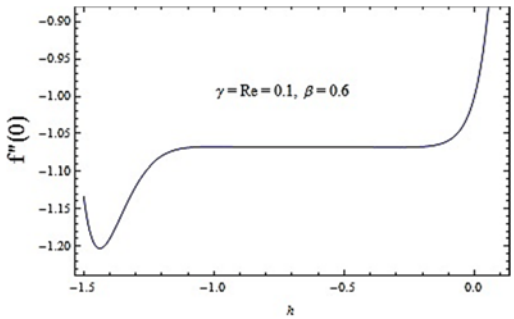

Fig. 3. $\hbar_f$ curve for velocity field.

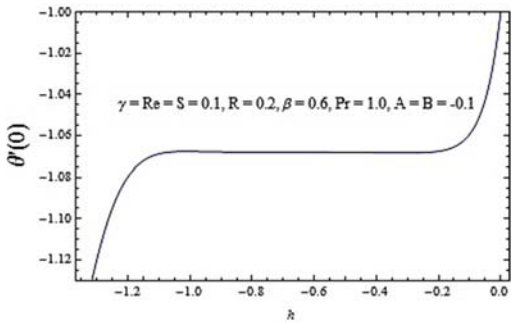

Fig. 4. $\hbar_\theta$ curve for temperature field.

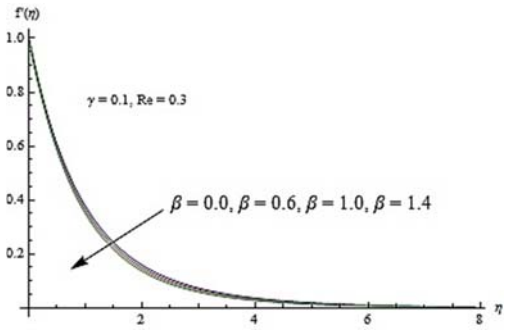

Fig. 5. Influence of β on velocity field.

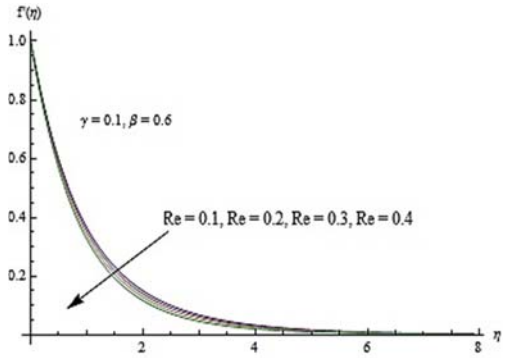

Fig. 6. Influence of Re on velocity field.

5. DISCUSSION

Study of different pertinent parameters on physical quantities of interest is presented in this section. Hence for this purpose we plot Figs. (5-15) for the velocity $f'(\eta)$ and temperature fields $\theta(\eta)$. Fig. 5 shows the influence of couple stress parameter β on the velocity field. It is clearly seen from this Fig. that the velocity field is decreasing function of β. In fact couple stress parameter depends upon the couple stress viscosity $\bar{\eta}$ and this couple stress viscosity acts as a retarding agent which makes the fluid more denser resulting into a decrease in the velocity of the fluid. Fig. 6 illustrates the effect of Reynolds number on $f'(\eta)$. As Reynolds number is the ratio of the inertia force due to wall stretching to the viscous force. Therefore for larger values of Reynolds number the velocity decreases to zero as $\bar{\eta}$ increases and flow decays very slowly to the ambient. Variation of the velocity field $f'(\eta)$ for different values of curvature parameter γ is displayed in Fig.7. Curvature parameter γ increases the velocity in the region $1 < \eta \leq 6$. Fig.8 depicts the effect of couple stress parameter β on the temperature field $\theta(\eta)$. Temperature profile and thermal boundary layer thickness are enhanced for larger values of β. Influence of Reynolds number on the temperature field is displayed in Fig. 9.

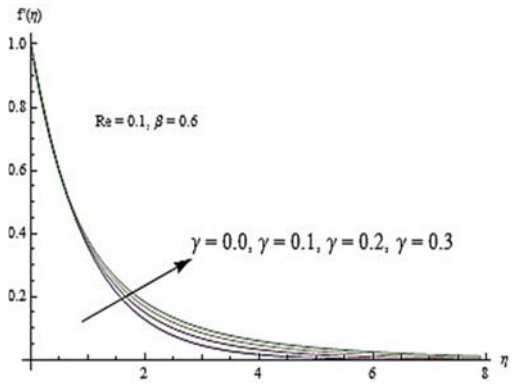

Fig. 7. Influence of γ on velocity field.

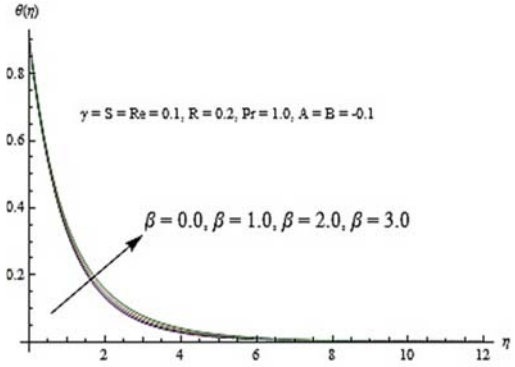

Fig. 8. Influence of β on temperature field.

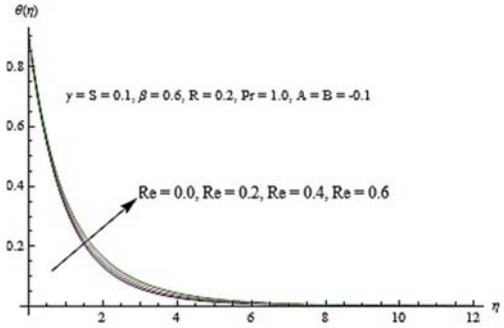

Fig. 9. Influence of Re on temperature field.

Table 1 Convergence of series solutions for different order of approximations when $\beta = 0.6$, $S = \mathrm{Re} = \gamma = 0.1$, $\mathrm{Pr} = 1.0$, $R = 0.2$, $A = B = -0.1$, $\hbar_f = -0.7$ **and** $\hbar_\theta = -0.8$.

Order of approximations	$-f''(0)$	$\theta'(0)$
1	1.0438	1.1224
5	1.0684	1.1304
10	1.0683	1.1306
15	1.0681	1.1307
20	1.0680	1.1308
25	1.0680	1.1308
30	1.0680	1.1309
35	1.0680	1.1309
40	1.0680	1.1309
45	1.0680	1.1309

It is noticed that enhancement in Reynolds number leads to increase in temperature and thermal boundary layer thickness. Fig. 10 shows the influence of curvature parameter γ on $\theta(\eta)$. Temperature rises significantly after some larger distance from the wall when γ increases. Fig. 11 plots the influence of S on the temperature field $\theta(\eta)$. It is observed that the temperature in the boundary layer decreases for larger values of stratification parameter. Physically this is due to the fact that buoyancy factor reduces within the boundary layer when we increase stratification parameter S. Also ambient thermal stratification causes a significant decrease in the temperature. The effect of thermal radiation parameter R on the temperature field is shown in Fig12. Temperature profile is increasing function of R. Increase in the thermal radiation parameter enhances the thermal boundary layer thickness. Fig.13 plots for the temperature field for different values of A. By analyzing the graphs it reveals that smaller values of A decrease the temperature field. Fig. 14 shows the effect of temperature dependent heat source/sink parameter B on $\theta(\eta)$. Temperature profile is decreasing function of B when $B < 0$. Here more energy is absorbed and in result the temperature significantly drops within the boundary layer. It is evident from Fig. 15 that the temperature field increases when A and B are positive (in case of internal heat generation). This is due to the fact that for larger values of A and B the thermal boundary generates the energy and this causes an increases in the temperature.

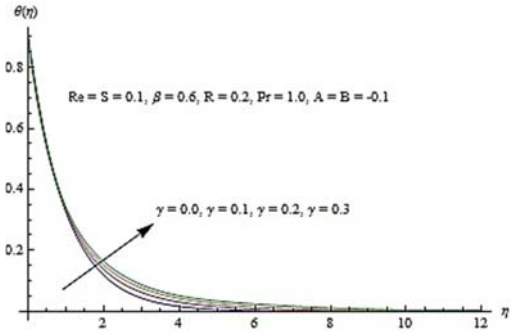

Fig. 10. Influence of γ on temperature field.

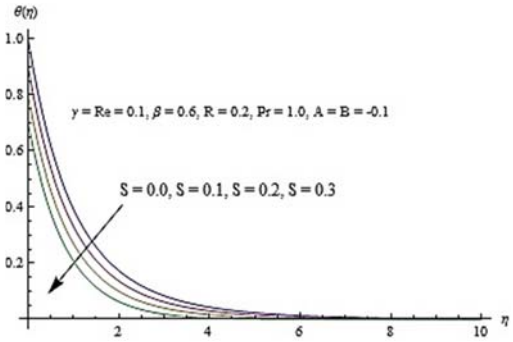

Fig. 11. Influence of S on temperature field.

Table 2 shows the numerical values of wall shear stress. This table indicates that the surface exerts drag force on the fluid. Enhancement in couple stress parameter (β), curvature parameter (γ) and Reynolds number (Re) lead to increase the magnitude of wall shear stress. Table 3 illustrates the effect of different physical parameter of interest on the Nusselt number. The fluid parameter (β) and stratification parameter (S) decrease the value of Nusselt number. Furthermore the Nusselt number for negative values of A and B (i.e. internal heat absorption) increases when compared with the positive values of A and B (i.e. internal heat generation). Also see Fig. (16-19)

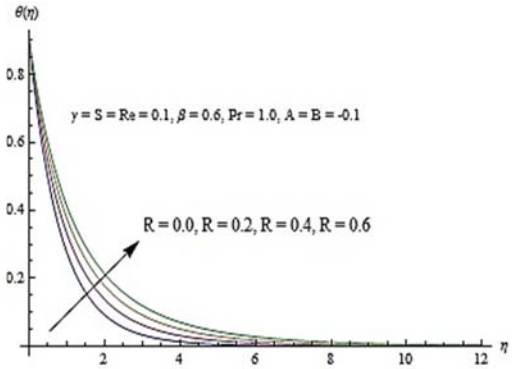

Fig. 12. Influence of R on temperature field.

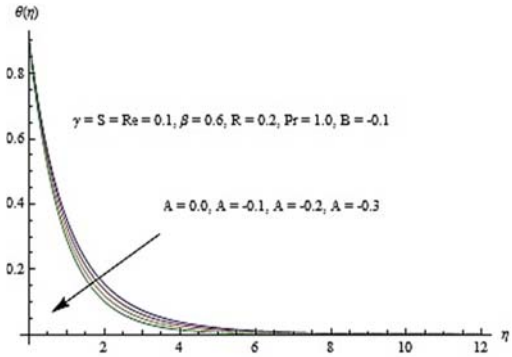

Fig. 13. Influence of A on temperature field.

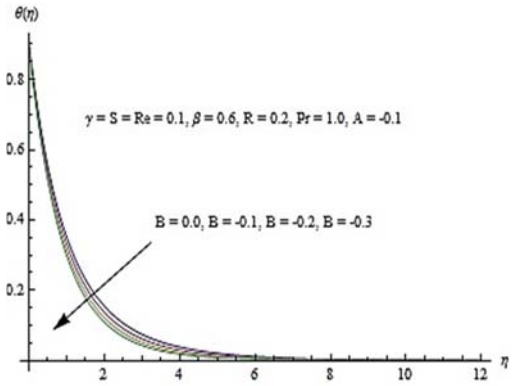

Fig. 14. Influence of B on temperature field.

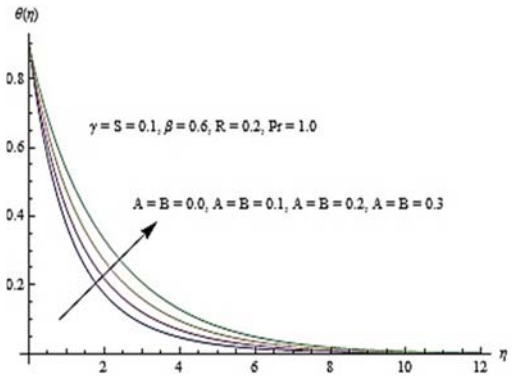

Fig. 15. Influence of A and B on temperature field.

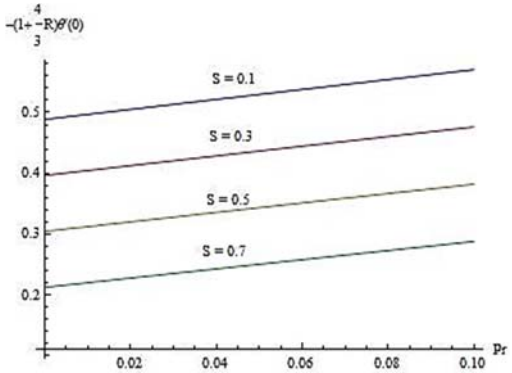

Fig. 16. Influence of S on Nusselt number.

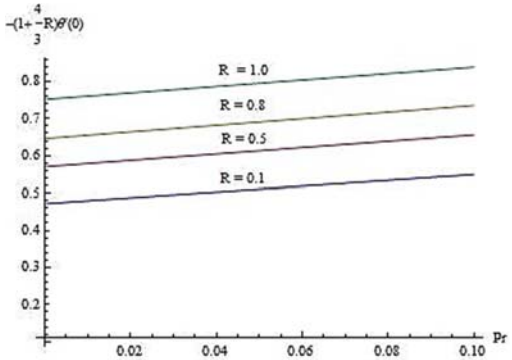

Fig. 17. Influence of R on Nusselt number.

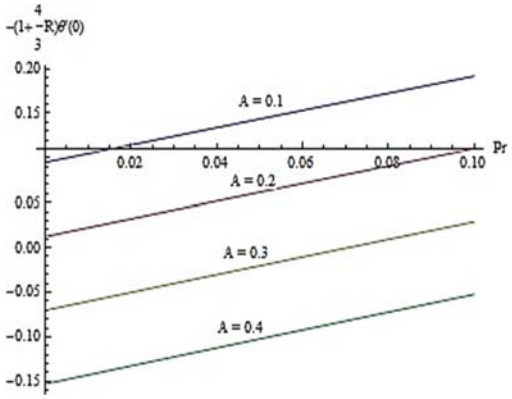

Fig. 18. Influence of A on Nusselt number.

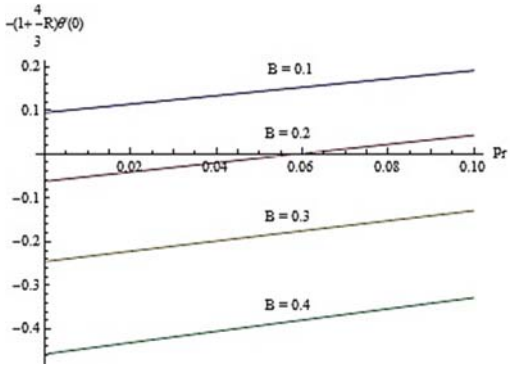

Fig. 19. Influence of B on Nusselt number.

Table 2 Values of wall shear stress for different parameters

β	γ	Re	$-f''(0)$
0.0			1.0366
0.4			1.0571
0.8			1.0796
0.6	0.0		1.0337
	0.1		1.0680
	0.15		1.0849
	0.1	0.0	1.0366
		0.12	1.0748
		0.13	1.0784

Table 3 Values of Nusselt number for different emerging parameters

β	γ	Re	R	Pr	S	A	B	$Re_x^{1/2}Nu_x$
0.0	0.1	0.1	0.1	1.0	0.1	-0.1	-0.1	1.2230
0.4								1.2159
0.7								1.2101
0.6	0.0							1.1609
	0.1							1.2121
	0.12							1.2221
		0.0						1.2229
		0.1						1.2121
		0.13						1.2083
			0.0					1.1058
			0.2					1.2119
			0.4					1.3030
				1.2				1.3328
				1.5				1.5004
				1.7				1.6046
					0.0			1.2669
					0.2			1.1572
					0.3			1.1022
						-0.1		1.2121
						0.0		1.1467
						0.1		1.0815
							-0.1	1.2121
							0.0	1.1502
							0.1	1.075

6. CONCLUSIONS

Effects of thermal radiation and non-uniform heat source/sink in flow of couple stress fluid by a stretching cylinder embedded in a thermally stratified medium are examined. Main findings of the presented analysis are mentioned below.

- Velocity $f'(\eta)$ decays for larger values of couple stress parameter β.
- Reynolds number Re increases the velocity and associated boundary layer thickness.
- Velocity and boundary layer thickness increase for larger curvature parameter.
- Effects of curvature parameter γ, couple stress parameter β and Reynolds number Re on the temperature field are qualitatively similar.
- Stratification parameter S decays the temperature and temperature gradient.
- Temperature and thermal boundary layer thickness increase when thermal radiation parameter R increases.
- Magnitude of wall shear stress increases through larger values of β, γ and Re.
- Nusselt number decays considerably when A and B increase.

REFERENCES

Bachok, N. and A. Ishak (2010). Flow and heat transfer over a stretching cylinder with prescribed surface heat flux. *Malaysian Journal of Mathematical Sciences* 4, 159-169.

Chamkha, J. A. (2011). Heat and mass transfer from MHD flow over a moving permeable cylinder with heat generation or absorption and chemical reaction. *Communication and Numerical Analysis* 2011, 20.

Chaudhary, S., S. S. Singh and S. Chaudhary (2015). Thermal radiation effects on MHD boundary layer flow over an exponentially stretching surface. *Applied Mathematics* 6, 295-303.

Daniel, S. Y. and K. S. Daniel (2015). Effects of buoyancy and thermal radiation on MHD flow over a stretching porous sheet using homotopy analysis method. *Alexandria Engineering Journal* 54, 705-712.

Ellahi, R, T Hayat, M. F. Mahomed and S. Asghar (2010). Effects of slip on the non-linear flows of a third grade fluid. *Nonlinear Analysis: Real World Applications* 11, 139-146.

Ellahi, R. and A. Riaz (2010). Analytical solutions for MHD flow in a third-grade fluid with variable viscosity. *Mathematics and Computational. Modelling* 52, 1783-1793.

Farooq, U., Y. L. Zhao, T. Hayat, A. Alsaedi and S. J. Liao (2015). Application of the HAM-based mathematica package BVPh 2.0 on MHD Falkner-Skan flow of nanofluid, *Computers & Fluids* 111, 69-75.

Gireesha, J., B. B. Mahanthesh, R. S. R. Gorla and T. P. Manjuntha (2015). Thermal radiation and

Hall effects on boundary layer flow past a non-isothermal stretching surface embedded in porous medium with non-uniform heat source/sink and fluid- particles suspension. *Heat and MassTransfer*.

Hayat, T., A. Qayyum and A. Alsaedi (2013). MHD unsteady squeezing flow over a porous stretching plate. *European Physical Journal Plus* 128, 157.

Hayat, T., S. Asad and A. Alsaedi (2014). Flow of variable thermal conductivity fluid due to inclined stretching cylinder with viscous dissipation and thermal radiation.*Applied Mathematics and Mechanics- English Editor* 35 , 1−12.

Hayat, T., S. Asad and A. Alsaedi (2014). Flow of variable thermal conductivity fluid due to inclined stretching cylinder with viscous dissipation and thermal radiation, *Applied Mathematics and Mechanics* 35, 717-728.

Hayat, T., S. Asad, A. Alsaedi and F. E. Alsaadi (2015). Radiative flow of Jeffrey fluid through a convectively heated stretching cylinder, *Journal of Mechanics* 31, 69-78.

Hayat, T., S. Asad, M. Mustafa and A. Alsaedi (2014). Radiation effects on the flow of Powell-Eyring fluid Past an unsteady inclined stretching sheet with non-uniform heat source/sink. *PLOS ONE* 9, e103214.

Hayat, T., S. Asad, M. Mustafa and A. Alsaedi (2015). MHD stagnation-point flow of Jeffrey fluid over a convectively heated stretching sheet, *Computers & Fluids* 108, 179-185.

Hayat, T., S. Asad, M. Mustafa and H. H. Alsulami (2014). Heat transfer analysis in the flow of Walters' B fluid with a convective boundary condition. *Chinese Physic B* 23, 084701.

Hayat, T., S. Asad, M. Qasim and A. A. Hendi (2012). Boundary layer flow of Jeffrey fluid with convective boundary conditions. *International Journal of Numerical Method Fluid* 69, 1350-1362.

Hayat, T., ShehzadA. S. Alsaedi A. and Alhothuali S. M.(2015). Three-dimensional flow of Oldroyd-B fluid over surface with convective boundary conditions, *Applied Mathematics and Mechanics-English Editor* 34, 489-500.

Jamil, M. Rauf A. Fetecau C. and Khan A. N, (2011). Helical flows of second grades fluid due to constantly accelerated shear stresses. *Communication in Nonlinear Science Numerical Simulation* 16, 1959-1969.

Khan, A., R. Ellahi, M. Gulzar and M. Sheikholeslami (2014). Effect of heat transfer on peristaltic motion of Oldroyd-B fluid in the presence of inclined magnetic field. *Journal of Magnetism and Magnetic Materials*372, 97-106.

Liao, J. S. (2009). Notes on the homotopy analysis method: Some definitions and theorems, *Communication in Nonlinear Science Numerical Simulation* 14, 983.

Maleki, M., S. A. M. Tonekaboni and S. Abbasbandy (2014).A homotopy analysis solution to large deformation of beams under static arbitrary distributed load. *Applied Mathematical Modelling* 38, 355-368.

Mukhopadhyay, S. (2012). Mixed convection boundary layer flow along a stretching cylinder in a porous medium. *Journal Petroleum Science Engineering* 08, 006 .

Mukhopadhyay, S. (2013). MHD boundary layer flow and heat transfer over an exponentially stretching sheet embedded in a thermally stratified medium. *Alexandria Engineering Journal* 52, 259-265.

Mukhopadhyay, S. (2013). MHD boundary layer slip flow along a stretching cylinder. *Ain Shams Engineering Journal* 4, 317-324.

Mukhopadhyay, S. (2015). Slip effects on MHD boundary layer flow over an exponentially stretching sheet with suction/blowing and thermal radiation. *Ain Shams Engineering Journal* 4, 485-491.

Mukhopadhyay, S. and A. Ishak (2012). Mixed convection flow along a stretching cylinder in a thermally stratified medium. *Journal of Applied Mathematics* 2012, 8.

Mukhopadhyay, S., D. P. Ranjan, K. Bhattacharyya and G. C. Layek (2013). Casson fluid flow over an unsteady stretching surface. *Ain Shams Engineering Journal* 4, 933-938.

Murthy, N. S. V. P., Ch. Reddy Ram, J. A. Chamkha and M. A. Rashad (2013). Magnetic effect on thermally stratified nanofluid saturated non-Darcy porous medium under convective boundary condition. *International Communication Heat Mass Transfer* 47, 41-48.

Paolucci, S. and J. Z. Zikoski (2013). Free convective flow from a heated vertical wall immersed in a thermally stratified environment. *InternationalJournal Heat Mass Transfer* 67, 1062-1071.

Patil, M. P., S. Roy and I. Pop (2012). Unsteady effects on mixed convection boundary layer flow from a permeable slender cylinder due to non-linearly power law stretching. *Computers &Fluids* 56, 17-23.

Rashidi, M. M., M. Ali, N. Freidoonimehr, B. Rostami and A. Hossian (2014). Mixed convection heat transfer for viscoelastic fluid flow over a porous wedge with thermal radiation, *Advance in Mechanical Engineering* 10.

Rostami, B.,M. M. Rashidi, P. Rostami, E. Momoniat and N. Rreidoonimehr (2014). Analytical investigation of laminar viscoelastic fluid flow over a wedge in the presence of buoyancy force effects. *Abstract and Applied*

Analysis 11.

Sahu, R. and K. S. Mishra (2015). Boundary layer flow and heat transfer of a dusty fluid over a vertical permeable stretching surface. *International JournalResearch Engineering Technology* 4, 2321-7308.

Sheikholeslami, M., R. Ellahi, H. R. Ashorynejad, G. Domairry and T. Hayat (2014). Effect of heat transfer in flow of nanofluids over a permeable stretching wall in a porous medium. *Journal Computational and Theoretical Nanosciences* 11, 486 – 496.

Turkyilmazoglu, M. and I. Pop (2013). Exact analytical solutions for the flow and heat transfer near the stagnation point on a stretching/shrinking sheet in a Jeffrey fluid. *International Journal Heat Mass Transfer* 57, 82 – 88.